ACS SyntheticBiology

Research Article

pubs.acs.org/synthbio

Engineering Integrated Digital Circuits with Allosteric Ribozymes for Scaling up Molecular Computation and Diagnostics

Robert Penchovsky*

Department of Genetics, Faculty of Biology, Sofia University "St. Kliment Ohridski", 8 Dragan Tzankov Blvd., 1164 Sofia, Bulgaria

Supporting Information

ABSTRACT: Here we describe molecular implementations of integrated digital circuits, including a three-input AND logic gate, a two-input multiplexer, and 1-to-2 decoder using allosteric ribozymes. Furthermore, we demonstrate a multiplexer−decoder circuit. The ribozymes are designed to seek-and-destroy specific RNAs with a certain length by a fully computerized procedure. The algorithm can accurately predict one base substitution that alters the ribozyme's logic function. The ability to sense the length of RNA molecules enables single ribozymes to be used as platforms for multiple interactions. These ribozymes can work as integrated circuits with the functionality of up to five logic gates. The ribozyme design is universal since the allosteric and substrate domains can be altered to sense different RNAs. In addition, the ribozymes can specifically cleave RNA molecules with triplet-repeat expansions observed in genetic disorders such as oculopharyngeal muscular dystrophy. Therefore, the designer ribozymes can be employed for scaling up computing and diagnostic networks in the fields of molecular computing and diagnostics and RNA synthetic biology.

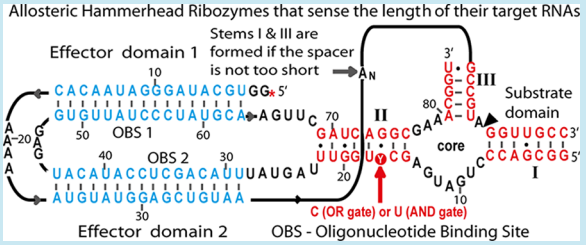

KEYWORDS: *allosteric ribozymes, RNA length biosensors, molecular electronics, integrated molecular circuits, molecular computation, self-assembly, nanodevices, molecular diagnostics, triplet-repeat expansion diseases*

Information processing is essential for any living cell as well as for any computing device. Therefore, engineering molecular computing systems may help us better understand and appreciate the information processing in the cell. Furthermore, this may allow us to create integrated nanodevices that can sense diverse signals and respond to them in a programmed mode. To design such devices, we have to integrate many functions into self-assembly structures built of various molecules. This is the way the cell executes information processing. The most complex information-processing structure in the cell is the ribosome built of various RNA molecules and proteins. Solving the three-dimensional structure of the bacterial ribosome provided us with ultimate details on the molecular function of this unique cellular machine.[1] In fact, the ribosome turned out to be a ribozyme since its enzymatic function is executed only by RNA molecules.[1,2] Nature has set RNA in the catalytic core of its most advanced cellular machine. That inspired us to research whether we can engineer nanodevices based on a self-assembly of RNA molecules. Such devices can work as integrated digital circuits and can be used for molecular electronics and diagnostics. The self-assembly of nucleic acids has been already employed for molecular computing.[3] However, the results of nucleic acids self-assembly are usually difficult for readout. Here, we aim to couple the nucleic acids self-assembly with producing of an output signal easy for readout.

The logic gate is the elementary building block of any digital circuit that is the backbone of modern electronics.[4] At any given time, every terminal of an electronic logic gate is in one of the two binary states either "0" or "1". Complex information-processing operations can be performed by building combinations of logic gates. According to the computational theory, there is no limit to the number of gates that can be arrayed together into a single device. In practice, however, the number of gates that can be assembled in a given physical space is limited.

In the past, the engineers faced the difficulties of building complex computing circuits by manually connecting single logic gates. This problem has been solved by the invention of the integrated circuit (IC) and its current development: the very large integrated circuit (VLIC). As a result, the required space for any type of digital circuit decreases enormously.[4] It is now believed that the silicon-etched technology will reach its physical limits within the next two decades.[5]

The first molecular computing was demonstrated by Leonard Adleman in 1994 using DNA strands to solve the seven-point Hamiltonian path problem.[6] Since then, one of the main fields of DNA computing is the development of nucleic acid-based electronics built by single logic gates that communicate to each other.[7−16] A landmark device was recently demonstrated with the functionality of a four-bit square root circuit that comprises 130 DNA strands.[17] The circuitry employed single DNA logic gates based on a reversible strand displacement. This provides, once again, strong evidence that nucleic acids can be used as

Received: June 12, 2012
Published: August 1, 2012

logic gates for building complex computing circuits that work in parallel.

At the same time, such research raises questions about the feasibility of building integrated molecular circuits (IMCs) with the complexity of electronic ones. The main building block of chemical circuitry can be the IMC similar to the IC. Despite the significant progress achieved recently in assembling various molecular circuits, no one has demonstrated any IMC like to silicon-based ICs in terms of functionality, reliability and complexity. Therefore, our abilities to build complex IC still need more research to improve their functionality as well as to expand their applications.

We demonstrate the feasibility of designing IMCs with allosteric riboswitches based on the hammerhead ribozyme (HHR). Ribozymes are natural RNA molecules with a catalytic function.[18] In nature, the HHR catalyzes its self-cleavage, although under single turnover conditions. Most hammerhead ribozymes are subsets of two classes of plant infective RNAs such as satellite RNAs of RNA viruses and viroids. Hammerhead ribozymes are also found in animals like the human pathogenic worm *Schistosoma mansoni*.[19] Designer HHR can be made to cleave external RNAs under multiple turnover conditions in response to ligand binding.

Allosteric ribozymes can be obtained by various methods, including *in vitro* selection,[20] rational,[21] and computational design.[22] We employ a proven and highly accurate algorithm for designing oligonucleotide-sensing allosteric switches.[22−24] Applying this technique in conjunction with the established RNA-length sensing feature, we demonstrate that it is possible to shrink a digital circuit with a functionality of five individual logic gates into a single catalytic RNA molecule. These RNA switches are used as a self-assembling platform for interactions with other DNA and RNA oligonucleotides.

This paper demonstrates that IMC can be built around single functional RNA molecules used as a platform for multiple interactions. Such assemblies can be used not only as nanodevices for scaling up molecular computation but also as convenient tools for molecular diagnostics. The RNA-length sensing features of these ribozymes can be used as an efficient method for diagnostics of a growing number of genetic disorders associated with various triplet-repeat expansions.[25,26] Designer ribozymes presented can distinguish between RNA molecules with a normal and mutant number of triplet-repeats observed in oculopharyngeal muscular dystrophy (OPMD) disorder.

METHODS

Computational Design of Oligonucleotide-Sensing Allosteric Ribozymes. The ribozyme designs employed in this paper were obtained by a computational algorithm for designing allosteric oligonucleotide-sensing ribozymes. The approach predicts the secondary structures based on the partition function of RNA folding in the presence and absence of effector molecules.[22] The partition function, in contrast to the minimal free energy function, computes the entire ensemble of all possible secondary structures as a function of temperature.[27] For this goal, the Vienna RNA folding package[28] and thermodynamic parameters[29] were used.

We employ the sequence of the AND gate (see point 1 below) to convert it into an OR gate by a single base substitution in stem II of the ribozyme using the algorithm described below. Four different states, namely, in the absence of any effector (an OFF state) and in the presence of one or both effectors (three ON states), were computed for each ribozyme. When the effector oligonucleotide is present, the complementary oligonucleotides of the ribozymes are excluded of the ribozyme folding because they are defined to have no binding properties. The procedure employs a random search algorithm as already described.[32] The computational steps were as follows (Figure S1, Supporting Information (SI)): (1) Substitute randomly one of the nucleotides shown below in the capital letters over the alphabet of A, U, C, G. 5′ggcgacccugaugag-CUUGGUUuaguauuuacagcuccauacaugagguguuaucccuaugcaa-guucGAUCAGGcgaaacggu. (2) Fold the sequence obtained and calculate the free energy at 37 °C of the structure using the partition function. (3) Determine whether nucleotides (from 8 to 14) of the hammerhead core participate in base pair formation in the dominant OFF state secondary structure using the probability dot matrix plot derived from the partition function. If one or more nucleotides 8 through 14 remain unpaired, reject the sequence and go to 1. (4) Replace the oligonucleotide binding site (OBS) 1 from the structure with the same number of artificial nucleotides that are defined to have no binding properties. (5) Fold the sequence and compute the free energies of this state based on the partition function. If a dominant ON state is not formed, go to 1. (6) Replace the OBS2 from the structure with the same number of artificial nucleotides that are defined to have no binding properties. (7) Fold the sequence and compute the free energies of this state based on the partition function. If a dominant ON state is not formed, go to 1. (8) Replace the OBS1 and OBS2 from the structure with the same number of artificial nucleotides that are defined to have no binding properties. (9) Determine if the resulting ON structure is dominating more than 80% and carries stem II that is required for function of the HHR by using the probability dot matrix plot derived from the partition function. If there is not a dominant structure, reject the sequence and go to 1. (10) Compute the free energy of the dominant OFF state secondary structure based on the partition function and determine the gap between the OFF and ON state free energies. If the energy gap is more than 15.0 kcal mol^{-1}, reject the sequence and go to 1.

Preparations of Nucleic Acids. The DNA oligomers were purchased from Integrated DNA Technology (Leuven, Belgium). The oligomers up to 40 nt in length were purified by HPLC. The longer oligomers were purified by denaturing (8 M urea) polyacrylamide gel electrophoresis (PAGE). For *in vitro* transcription, two overlapping DNA strands (template and nontemplate) were made double-stranded (ds) by extension with SuperScriptII reverse transcriptase (Invitrogen, Carlsbad, CA) according to the manufacturer's instructions. The nontemplate strand carried a T7 RNA polymerase promoter (TAATACGACTCACTATA). The dsDNAs obtained were precipitated with ethanol and used as templates for *in vitro* transcription with a RiboMax kit (Promega, Madison, WI). The transcribed RNAs were purified by 6% denaturing PAGE. Fluorescent labeling at the 5′-terminus was achieved during transcription in the presence of 5′-FAM-ApG, purchased from IBA (Göttingen, Germany).

Allosteric Ribozyme Assays. Allosteric ribozymes (200 nM) were incubated in a solution containing 50 mM Tris-HCl with pH 8.5 at 37 °C), 50 mM KCl, and 20 mM $MgCl_2$. Ribozyme reactions were initiated by adding target RNA molecules (typically to a final concentration of 80 nM) at 37 °C. In some cases, the target RNAs were previously melted at 93 °C for 1 min in the presence of cDNA oligomers (200 nM)

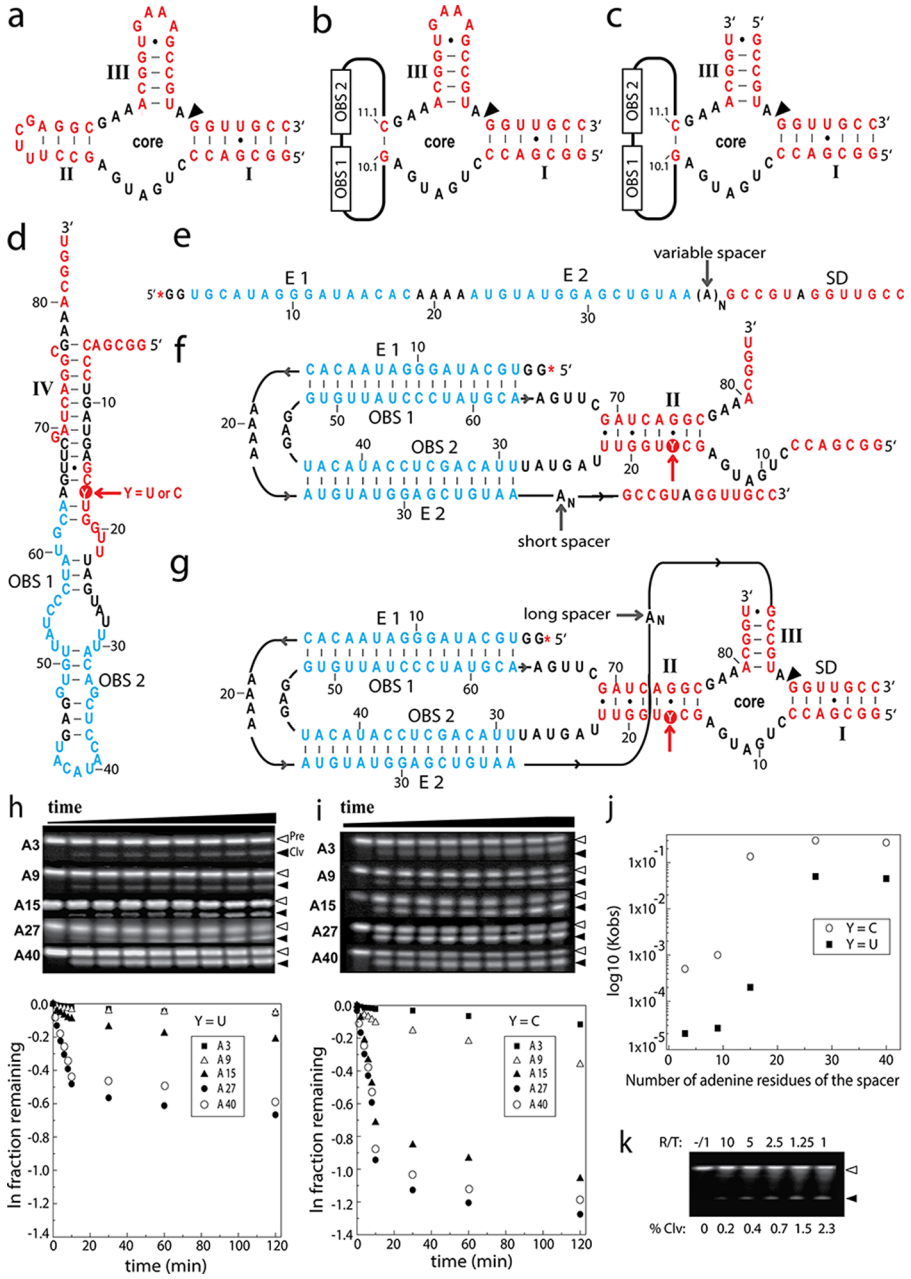

Figure 1. Allosteric ribozymes that can sense the length of their substrate RNA molecules. (a) Minimal version of the parental hammerhead ribozyme (HHR) used in the current study. Stems I through III (red) have to be formed for self-cleavage of the ribozyme at the position indicated by the black arrowhead. (b) Embedding two oligonucleotide binding sites (OBS 1 and 2) into stem II of the parental HHR. (c) The oligonucleotide-sensing HHR is modified to cleave external RNA molecules. (d) Allosteric ribozymes designed to cleave external RNA molecules carry two OBS 1 and 2 (blue). The ribozymes differ in one base indicated by the red arrow (Y = U or C). In the absence of effector, the ribozymes fold into an inactive conformation by forming stem IV. The ribozyme with a U base has AND logic function, while that with a C base is an OR gate. (e) The target RNA molecules have two effector domains (E1 and E2, blue nucleotides), complementary to the OBS1 and 2 of the ribozymes, a substrate domain (S, red), and a variable spacer built of a different number (N) of adenine residues (AR). The target RNAs are 5′-FAM-ApG labeled as indicated by the star (*). (f) If the spacer of the target RNA is too short, the core of the ribozyme is not formed, and the substrate RNA is uncleaved. (g) When the variable spacer is long enough, all three stems (in red) are formed, and the substrate RNA is cleaved at the position indicated by the arrowhead. (h) Gel images of cleavage kinetics of 5′-FAM-ApG labeled RNA molecules with five different numbers (A = 3, 9, 15, 27, and 40) of ARs are cleaved by the AND-ribozyme under single turnover conditions. The fragments cleaved (Clv) are separated from the precursors by denaturing PAGE. A plot, using data derived from the gels, depicts the natural logarithm of the remaining fraction of noncleaved RNA versus time for the target RNAs. (i) The same contents like this presented in (h) but for the OR-ribozyme instead of the AND-ribozyme. (j) Log_{10} of the cleavage kinetics as a function of different number adenine residues of the variable spacer for both ribozymes. There is about a 200-fold difference in the rate constants of cleavage between the target molecules with 9 AR and those with 15 for the OR-ribozyme and about 250 fold difference between 15 and 27 AR for the AND-ribozyme. (k) A gel image of cleavage of a target molecule without any spacer under various concentration ratios between the target RNA and the AND-ribozyme is demonstrated.

dx.doi.org/10.1021/sb300053s | ACS Synth. Biol. 2012, 1, 471−482

and incubated at a room temperature for 5 min. In the case to the multiplexer−decoder circuit, the S1 or S2 target molecules were incubated first in the OR-ribozyme for 30 min. After that, the labeled NOT or YES ribozymes were added each at concentration of 200 mM and incubated for the additional 30 min.

The ribozyme reactions were stopped by adding an equal volume of gel loading buffer containing 100 mM EDTA, pH 8.5. The reaction products were run on 6% denaturing polyacrylamide gel electrophoresis (PAGE). The 5′-FAM-labeled RNAs from the gels were detected using a blue-light transilluminator, DarkReader-195 M (light length from 400 to 500mn) from Clare Chemical Research, Inc. (Dolores, CO) and Nikon D5100 digital camera (Nikon Imaging Japan Inc., Tokyo, Japan) equipped with a 520 nm optical filter. The images were analyzed with the ImageJ software (NIH, Bethesda, MD).

RESULTS AND DISCUSSION

Design and Experimental Validation of RNA Length Sensing Ribozymes. Proteins and RNAs can exhibit not only catalytic but also a complex allosteric function alike. All molecular switches presented throughout this work are based on the HHR. The minimal version of the HHR, required for its catalytic function, is depicted in Figure 1a. All three stems (from I to III) have to be properly formed to propagate the ribozyme's self-cleavage. Thus, the HHR has to fold into specific secondary (Figure 1a) and tertiary structures to function as an enzyme. Variants in primary sequence that preclude formation of this secondary structure will result in reducing enzymatic activity or complete inactivity.

In this study, we design allosteric ribozymes by embedding two OBSs into stems II or III of the HHR. The allosteric ribozymes presented throughout this paper are designed to undergo a swift folding change that alters the ribozyme's function in response to ligand binding by a highly accurate computational algorithm described in the Methods and depicted in Figure S1 (SI). The ribozymes can be engineered either to cleave themselves (Figure 1b) or to cleave an external RNA (Figure 1c). The allosteric ribozyme has two main functions: molecular recognition, and conformational and functional switching between OFF and ON states depending on their logic properties. The ribozyme design presented is general since the allosteric and substrate sites can be altered in regard to a particular application. The ribozymes were computationally designed to carry two OBSs, which can bind two effector oligomers. In the absence of any effectors, the ribozymes are predicted to fold into a dominant secondary structure that is an enzymatically inactive (OFF) state (Figure 1d). The allosteric ribozymes, shown in this paper, have an additional feature to sense the length of their target RNA molecules. These ribozymes are capable of simultaneously recognizing four predefined domains of a target RNA molecule: two allosteric, one substrate, and one spacer domain (Figure 1e).

The AND-ribozyme was previously designed to serve as a two-input AND gate that cleaves itself. In the absence of any or in the presence of one of the effectors, this AND-ribozyme is predicted to fold into dominant inactive state in which stem IV is formed instead of stem II. This is thermodynamically projected by the dot matrices of the partition function (Figure S2a,b,c (SI)). The ribozyme is designed to adopt an active state with a formation of stem II only in the presence of both effectors, which makes it a two-input AND logic gate (Figure S2d (SI)). Here, this ribozyme is designed to cleave external RNA molecules instead of cleaving itself and to sense their lengths (Figure 1f and d).

We used the sequence of the AND-ribozyme as a template for a computational selection of a ribozyme with an OR logic function by a single base substitution in stem II. All possible combinations of base substitutions in stem II were computationally tested by the algorithm described in the Methods and schematically depicted in Figure S1 (SI). The algorithm computes four different states using the partition function for RNA folding. It weights up all possible secondary structures. It aims to find dominant structures of at least 80% for all four states. In contrast to the AND-HHR, the OR-ribozyme was computed to have three dominant ON states in the presence of either (Figure S2f,g (SI)) or both effectors (Figure S2h (SI)), and one dominant OFF state in the absence of any effector (Figure S2e (SI)).

According to the algorithm employed, there was the best substitution of the U base at the 17th position with a C base (Figure 1d). The single point mutation was predicted not only to convert the AND logic function of the ribozyme into an OR function but also to increase the efficiency of cleavage by stabilizing the ON state (stem II, red nucleotides, Figure 1f,g) in the presence of either or both effectors (Figure S2 (SI)). The thermodynamic stability of the AND-ribozyme based on the partition function (E_p = −25.79 kcal mol^{-1}) is only 12% higher than that of OR-ribozyme (E_p = −22.69 kcal mol^{-1}) in the OFF state (Figure 1d). However, this has a significant effect on the cleavage efficiency as demonstrated below in this paper.

We demonstrate experimentally how the length of the target RNAs influences the cleavage efficiency. For this goal, target RNAs with various numbers (N) of adenine residues (AR) were enzymatically synthesized and 5′-FAM-ApG labeled as described in the Methods. The target molecules contain the same effector and cleavage domains complementary to the corresponding ribozyme sites (Figure 1e). They only differ in the space's length. All adenine-containing intervening sequences are not predicted to form any secondary structures. Therefore, the cleavage efficiency of the target RNAs, in this case, depends primarily on the length (the number of AR) of their variable spacers.

To establish the minimum spacer length of a target molecule needed for the most efficient cleavage by the AND-ribozyme in the presence of both effectors, we used five RNA molecules with different spacer length (ARs = 3, 9, 15, 27, 40) substrates. The reactions were carried out under single turnover conditions as described in the Methods. The gel images obtained for the cleavage kinetics of the target RNAs are shown in Figure 1h. The natural logarithm (ln) of fraction remaining of the ribozyme versus time is plotted in this figure. The curves for the target molecules with 3 and 9 ARs are completely overlapping and have the lowest rate constant of cleavage (k_{obs} = 2 × 10^{-5} min^{-1}). The target molecule with 15 ARs exhibits a rate constant of cleavage of about 2 × 10^{-3} min^{-1}. The RNAs with 27 and 40 ARs had the fastest cleavage kinetics of 5 × 10^{-2} min^{-1} and 4.5 × 10^{-2} min^{-1}, respectively, and cleavage efficiency of ca. 60% (Figure 1h). These results are very consistent with the predicted ca. 60% probability of forming ON (stem II) and 40% of OFF state (stem IV) in the presence of both effectors (Figure S2 (SI)) for the AND-HHR. The results obtained indicate a clear dependence between the length and the cleavage efficiency of the target molecules. There is

about a 250-fold difference in the rate constants of cleavage between the target molecules with 27 or 40 ARs and these with three ARs and about a 25-fold difference with target molecules that had 5 or 9 ARs (Figure 1j).

The same experiments were repeated with the OR-HHR (Figure 1i), which was predicted to form a dominant ON state in the presence of either or both effectors (Figure S2 (SI)). The OR-ribozyme was designed to have higher cleavage efficiency than that of U-ribozyme because its ON state was predicted to be ca. 80% dominant over all other possible secondary structures (Figure S2 (SI)). The same target molecules with spacers containing different numbers of AR were used. The images of the cleavage kinetics are shown in Figure 2i. The curves of the target molecules with 3 and 9 AR are very similar and indicate rate constants of cleavage $k_{obs} = 5 \times 10^{-4}$ min^{-1} and $k_{obs} = 1 \times 10^{-3}$ min^{-1}, respectively. In this case, the target molecule with a spacer of 15 AR exhibits a much higher rate constant of cleavage (2×10^{-1} min^{-1}) than that with the AND-ribozyme. Again, the targets with 27 and 40 ARs had the fastest cleavage kinetics of 3×10^{-1} min^{-1} and 2.6×10^{-1} min^{-1}, respectively, with cleavage efficiency of ca. 80% (Figure 2i).

The obtained results correspond very well with the theoretical predictions for the formation of one dominant ON state in the presence of both effectors (Figure S2 (SI)). As observed with the OR-ribozyme, there is a clear dependence between the length and the cleavage efficiency of the target molecules, although shifted to shorter spacer lengths. There is about a 200 fold difference in the rate constants of cleavage between the target molecules with 9 ARs and these with 15 ARs (Figure 2j). In addition, the cleavage yield of a molecule without any spacer between (AR = 0) was investigated under various concentration ratios between the target molecule and the AND-ribozyme. A cleavage of 0.4% was observed under ratio 5:1 in favor of the ribozyme and 2.3% only under ratio 1:1 (Figure 2k). The experimental results obtained by a fluorescence resonance energy transfer (FRET) method indicated complete inactivity for both ribozymes in the presence of 11 nt long DNA effectors compared to full activation with 16 nt long DNAs (Figure S3 (SI)).

The conclusions that can be drawn from these results are as follows. First, the hybridization of the target RNA molecule either to the ribozyme effector domain or to cleavage site is not sufficient to trigger the cleavage. Second, the lack of a spacer or the presence of a short spacer does not allow simultaneous interaction of the target molecule to the allosteric and substrate sites of the ribozyme. The experimental results are consistent with the theoretical predictions in terms of cleavage efficiency and logic function of the ribozymes. As computationally predicted, the OR-ribozyme with the C substitution makes the ON state more stable in the presence of both effectors (faster folding K_{on} and slower K_{off} of stem II) than AND-ribozyme. As a result, the effector molecules have more time to interact with the cleavage site of the OR-ribozyme forming an active conformation even with shorter spacers compared to the AND-ribozyme. The difference in the rate constants of cleavage for target RNAs with different length can be explained with a different degree of stability between the ON states of the two ribozymes.

Ribozyme Detection of RNAs with Triplet Repeats Observed in OPMD Disorder. At least 22 genetic disorders are known to be caused by repeat expansions in the human genome.[33] Thirteen of them are assumed to be caused by codon expansions in different genes. They can be categorized

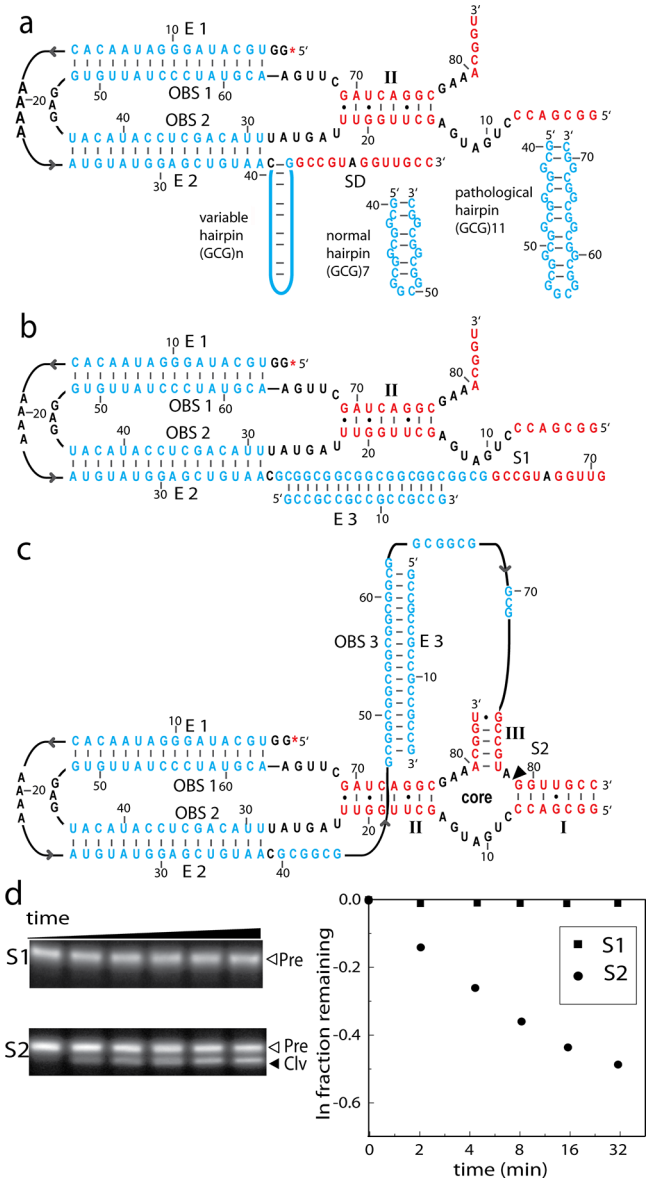

Figure 2. Ribozyme detection of RNAs with triplet repeats observed in the OPMD disorder. (a) Two target RNAs were enzymatically synthesized and 5′-FAM-ApG labeled as indicated by the star (*). Both targets have two effector sites (E1 and E2, blue), a variable hairpin (blue), and a substrate domain (red). One RNA has a normal number of 7 GCG repeats, while the other has 11 triplet repeats observed in the OPMD disorder. The AND-ribozyme is employed to interact specifically with both target molecules. However, in the absence of antisense oligonucleotide that opens the hairpins, the ribozyme cannot cleave its substrate RNAs because stems I and III are not formed. (b) The target RNA with the normal number of 7 GCG repeats is not going to be cleaved even in the presence of a hairpin antisense oligonucleotide because it is too short to form stems I and III. (c) The target RNA with the pathological number of 11 GCG repeats is long enough to form stems I and III in the presence of a hairpin antisense oligonucleotide. (d) Gel images of cleavage kinetics for the target RNAs in the presence of the AND-ribozyme and the hairpin antisense oligonucleotide. Left: As expected, the short RNA target with the normal number of 7 GCG repeats is not cleaved at all over 32 min. Right: In contrast, the long RNA target with the pathological number of 11 GCG repeats is cleaved at about 45% over 32 min. The results are plotted as a natural logarithm of fraction remaining versus time.

dx.doi.org/10.1021/sb300053s | ACS Synth. Biol. 2012, 1, 471−482

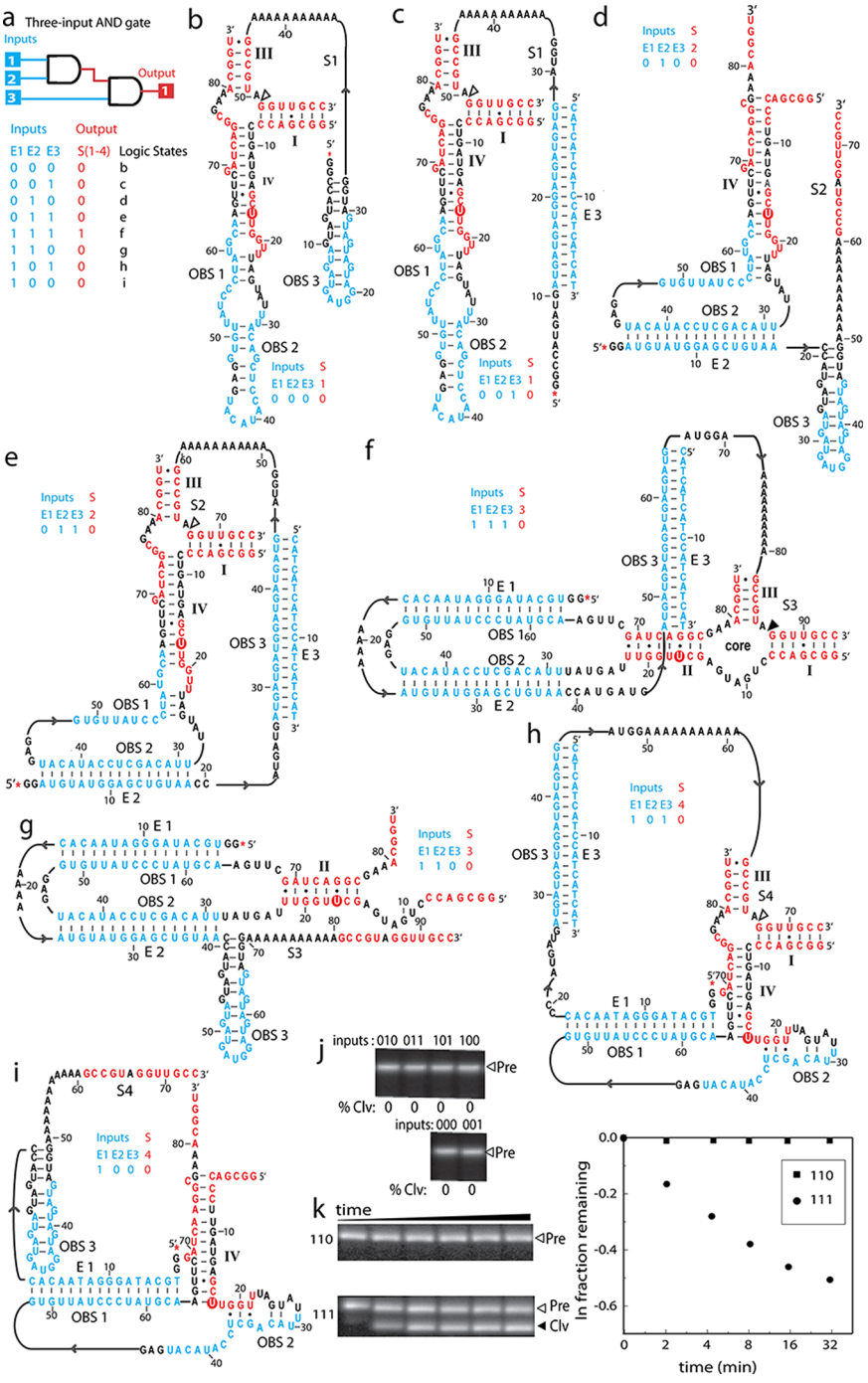

Figure 3. Integrated three-input AND gate. (a) An electronic three-input AND gate is usually implemented by a cascade connection of two AND gates each with two inputs. The truth table of three-input AND gate is shown. There are three inputs (blue) and one output (red) signals and 8 possible logic states. The output signal is "1" only when all three input channels have value "1". Otherwise the output signal is "0". (b) A RNA length-sensing AND-ribozyme was used to build a three-input AND-gate. The ribozyme has two oligonucleotide-binding sites (OBS1 and OBS2, blue). The OBS3 is a hairpin designed to be a part of the target RNA, which is 5′-FAM-ApG labeled as indicated by the red star (*). In the presence of a S1 target RNA, which carries a substrate domain (in red) and OBS3 (in blue), the ribozyme folds into an inactive conformation in which stem IV is formed instead of the natural stem III. (c) The ribozyme stays inert in the presence of the S1 target and third effector (E3), which is complementary to the hairpin structure (OBS3). (d) In addition to the sequence of S1, the S2 RNA carries the E2 effector. As a result, the ribozyme folds into an idle state. (e) The inactive state of the ribozymes with the S2 RNA is not activated even in the presence of the E3. (f) The S3 RNA carries E1 and E2 effector domains. In the presence of the E3 DNA oligomer, the AND-ribozyme folds into active conformation in which stems I, II, and III are formed. Therefore, the S3 target is going to be cleaved. (g) In the absence of E3, however, the S3 RNA cannot be cleaved, the OBS3 hairpin is formed, and stems I and III of the ribozyme are not present. (h) The ribozymes stay in an inactive conformation in the presence of S4 RNA and E3 effector. The S4 target lacks the E2 effector domain. (i) The S4 is not supposed to be cleaved by the ribozyme in the absence of E3 as well. (j) The target RNAs S1(000 and 001), S2(010 and 011), and S4 (100 and 101) are not cleaved by the ribozyme in various input combinations over 30 min as indicated by the denaturing PAGE gels. (k) Kinetics of cleavage of the S2 target RNA by the AND-ribozyme are presented in the absence (110, no cleavage) and in the presence (111) of the E3 oligomer. As expected, the cleavage is about 50% over 30 min.

dx.doi.org/10.1021/sb300053s | ACS Synth. Biol. 2012, 1, 471−482

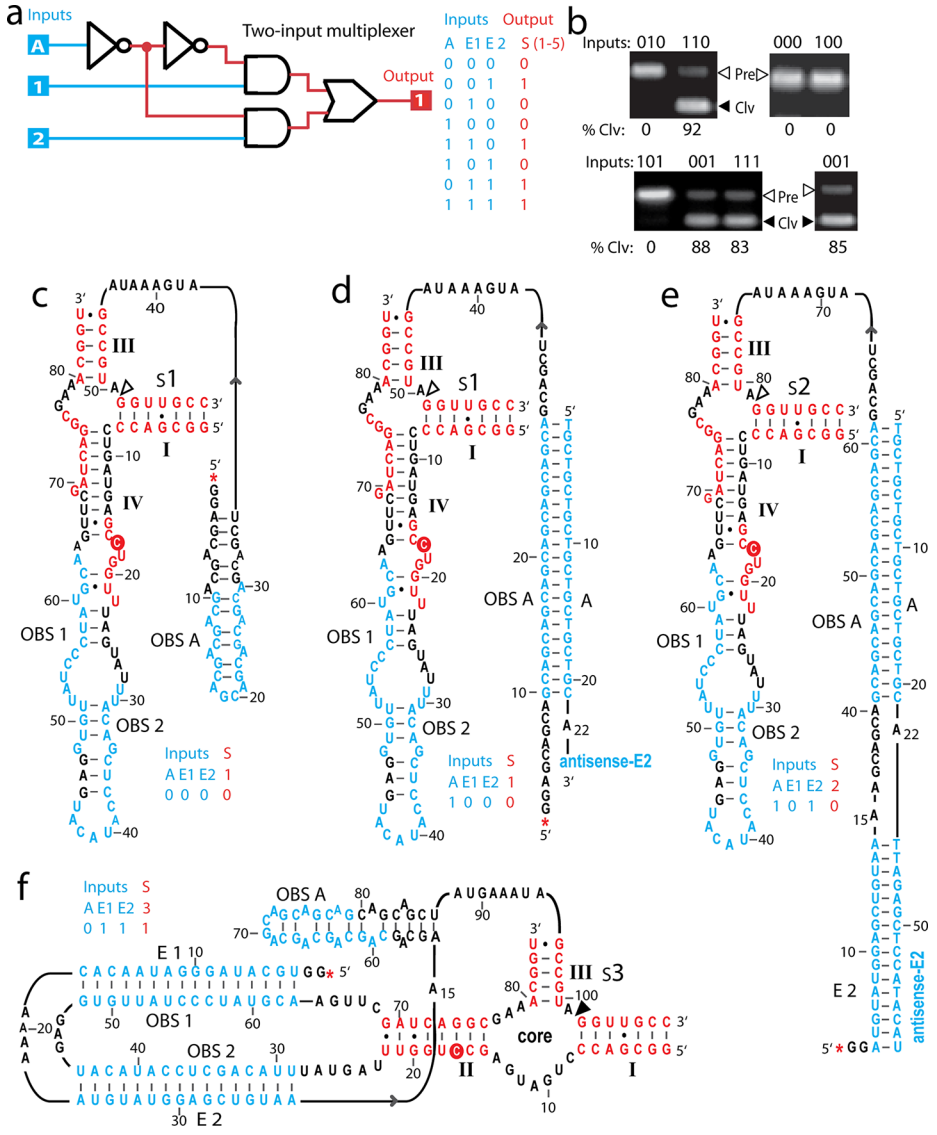

Figure 4. Integrated two-input molecular multiplexer circuit. (a) An electronic two-input multiplexer is usually implemented by a circuit of five logic gates. There are two data (1 and 2) and one register (A) inputs (blue) and a single output (red). The truth table of the multiplexer is shown. There are eight possible states, as half of them have a "1" value and the other half have a "0" value. (b) Denaturing PAGE gel images of 5 RNA target molecules, in the presence of the OR-ribozyme, are shown after incubation for 30 min. Each target RNA was 5′-FAM-ApG labeled. All logic states of the multiplexer were tested, as the cleaved and intact RNA targets exactly correspond to the truth table of the multiplexer in terms of input as well as output (cleaved or intact RNAs) signals. For more details for a particular logic state, see the legend below as well as Figure S4 (SI). (c) The OR-ribizyme was used to execute the function of the molecular multiplexer. In the presence of S1 RNA, which carries a substrate domain (in red) and a hairpin (OBS A, in blue), the ribozyme folds into an idle state. (d) The ribozyme stays inactive in the presence of S1 RNA and A DNA oligomer, which carries complementary domains to the OBS A and E2 effector with a spacer of 22 adenine bases between them. (e) In addition to the sequence of S1, the S2 target RNA carries an E2 effector domain. The ribozyme cannot cleave the S2 RNA in the presence of the A DNA effector because its E2 domain is complementary to the antisense site of DNA. (f) The S3 RNA carries E1 and E2 effectors as well as a spacer built of 15 adenine bases. As a result, all three stems required for the ribozyme function are formed, and the S3 RNA has to be cleaved. For the other 4 logic states of the molecular multiplexer, see Figure S4 (SI).

into polyglutamine, such as Huntington's disease, and polyalanine disorders. Many of the repeat expansion disorders are lethal at a certain age. In addition, most of them are difficult to diagnose and impossible to cure. The formation of stable DNA and RNA hairpins observed in most of these diseases complicates their molecular identification.

Expansion of polyalanine tracts in the gene that encodes the human polyadenylate-binding nuclear protein 1 (PABPN1) is the cause for the already mentioned OPMD disorder. The PABPN1 is an abundant nuclear protein that binds with high affinity to nascent poly(A) tails of pre-mRNAs. This protein is required for progressive and efficient polymerization of poly(A) tails to about 250 nt on the 3′-ends of mRNA. The poly(A) tail is essential for the stability of any eukaryotic mRNA. An expansion of the GCG codon from normal 7 to 10−17 at the 5′-end of the coding region of this gene leads to the autosomal dominant OPMD disease.

Here, we demonstrate that an RNA length sensing ribozyme can be used to distinguish between a normal and pathological number of GCG repeats observed in OPMD disease using a model system that fits to our ribozyme. The OBS of the ribozyme can be easily adapted to any sequence of interest.

dx.doi.org/10.1021/sb300053s | ACS Synth. Biol. 2012, 1, 471−482

Two target RNAs are synthesized and labeled as described in the Methods. One of the RNAs carries a spacer built of $(GCG)_7$, while the other RNA has $(GCG)_{11}$ repeats (Figure 2a). Both substrate RNAs are incubated with the AND-ribozyme in the presence of hairpin antisense DNA oligomers over 20 min under standard conditions (Figure 2b,c). As expected, a small amount of cleavage (7%) was observed with the $(GCG)_7$ RNA, while the $(GCG)_{11}$ RNA was cleaved at 50% (Figure 2d). These results suggest that we can apply RNA-length sensing ribozymes for molecular detection of OPMD disorder.

It is well-known that triplet repeats tend to form stable hairpin structures both *in vitro* and *in vivo*. The formation of such hairpins obscured the length differences of these molecules and made impossible specific cleavage based on the number of triplet repeats. However, upon addition of antisense oligomers, the hairpins can be opened, and the ribozyme can selectively cleave its target RNAs based on the number of their repeats. Therefore, the ribozyme design described here can be employed as a tool for detection of RNAs with various triplet repeat expansions.

Moreover, we speculate that such ribozymes may be of interest as a model for developing cellular detection arrays as well as gene therapy based approaches for specific down regulation of PABPN1 mRNA with pathological GCG expansions. A HHR based on the minimal version, similar to the ribozyme shown in this paper, was already used in cells to cleave mRNA with triplet repeat expansions, however, without any length discrimination.[30] Although, a variety of approaches for specific knockdown of mRNAs have been developed based on antisense, ribozyme, and RNA interference mechanisms, none of these tools have been used specifically to cleave RNA depending on its length.

Integrated Three-Input Molecular AND Gate. In electronics, three-input AND gate is usually implemented by a digital circuit of two cascade AND gates each having two inputs (Figure 3a).[4] The output signal of the gate is positive only in the presence of the three input signals as shown in the truth table in Figure 3a. In this section, we demonstrate an IMC that executes the logic of three-input AND gate using a single allosteric ribozyme. We employed the AND-ribozyme (Figure 1) that is a two-input AND gate with two OBSs as already described. It forms a dominant stem III only in the presence of both effectors (Figure S2d (SI)). To use this ribozyme as a three-input logic gate, we employed its RNA length-sensing feature demonstrated in the previous sections. For this goal, four target RNA molecules were enzymatically synthesized and 5′-FAM-ApG labeled as described in the Methods. All target RNAs consist of a hairpin and a substrate domain, in red (Figure 3). The target S1 does not have any effector domains. The target molecules S2, S3, and S4 differ in their effector sites, which can contain either one or both effectors (Figure 3).

We tested all eight logic states of the ribozyme-based tree-input AND gate (Figure 3). The reactions described in this section are incubated for 30 min under standard conditions detailed in the Methods. In the presence of the target S1, which lacks the second effector site (E2), the ribozyme is designed to fold into an inactive state even in the presence of the third effector (E3) that is complementary to the hairpin sequence. The oligonucleotide E3 opens the hairpin and allows the formation of stems I and III, but stem IV is still present (Figure 3c) due to the lack of E2 effector. This prediction is experimentally proven in Figure 3h. If the missing E2 is added as a separate a DNA sequence (D2, Figure 3a), the S1 is cleaved as expected (Figure 3h). In this state, all input signals are present. The S2 target has E2 domain but lacks E1. Even in the presence of the antihairpin DNA (E3) the stem IV is still formed (Figure 3d), and the target molecule is not cleaved (Figure 3h). Only after the addition of DNA oligomer (D1) that is complementary, the OBS1 the cleavage of S1 is observed (Figure 3h). If the S3 is present, the ribozyme is supposed to form stem II (Figure 3e). However, a cleavage of the S3 is observed only in the simultaneous presence of E3 as shown in Figure 3g.

All results obtained represent exactly the logic function of a three-input AND Boolean logic gate. In contrast to the electronic implementation, we have replaced the two electronic AND gates with one allosteric ribozyme, which senses the length of its target molecules. Note that the OBS and the cleavage site of the ribozyme can easily be changed by a fully computerized procedure as previously described. These three-input molecular AND gates can be designed to work in parallel in contrast to the previously described chemical three-input AND gate.

Integrated Two-Input Molecular Multiplexer. A multiplexer is a digital device with several signal inputs and a single output. One particular input is selected by the address input to be sent to the singular output.[4] A typical implementation of an electronic two-input multiplexer and its truth table are depicted in Figure 4a. This device is also known as a time-division multiplexer. It features an electronic scheme of five logic gates: two with NOT and AND logic functions and one with OR logic. The input A is the addressing register that controls which one of the two data inputs, either 1 or 2, will be propagated to the output. If the register input switches forward and backward at a frequency more than double that of either data inputs, both data signals can be transmitted in parallel.

In this study, we demonstrate that the OR-ribozyme can be used as an integrated two-input multiplexer. In contrast to the electronic version, where an integrated circuit of five gates is applied (Figure 4a), our molecular version is based on the function of a single type allosteric ribozyme (Figure 4). For this aim, we employed the RNA length sensing feature of the OR-ribozyme described in the previous sections (Figure 1).

To implement the complete functionality of a two-input molecular multiplexer device, we enzymatically synthesized and 5′-FAM-ApG labeled five target RNA molecules, from S1 to S5 (Figures 4 and S4 (SI)) as described in the Methods. The ribozyme assays were performed for 30 min under standard conditions if not stated otherwise. We experimentally tested all logic states of the multiplexer. All target RNAs have a hairpin domain that is the binding site for the addressing input, OBS A, as well as a substrate domain that binds to the ribozyme, in red (Figures 4 and S4 (SI)).

The S1 target has no effector domains and is not cleaved by the OR-ribozyme even in the presence of an addressing oligonucleotide (A) that opens the hairpin (Figure 4b,c,d). In addition, the A oligonucleotide carries an antisense sequence to the oligonucleotide effector E2. As a result, the target S2, which carries the E2 domain, stays intact in the presence of the addressing effector (Figure 4b,e). The S3 RNA consists, in addition, of E1 and E2 domains, a spacer built of 15 adenine bases. It activates the ribozyme due to the formation of stems from I to III (Figure 4f). As a result, the S1 is cleaved about 91% (Figure 4b). The S4 target RNA differs from the S3 with the absence of the E1 domain. However, it is cleaved by the

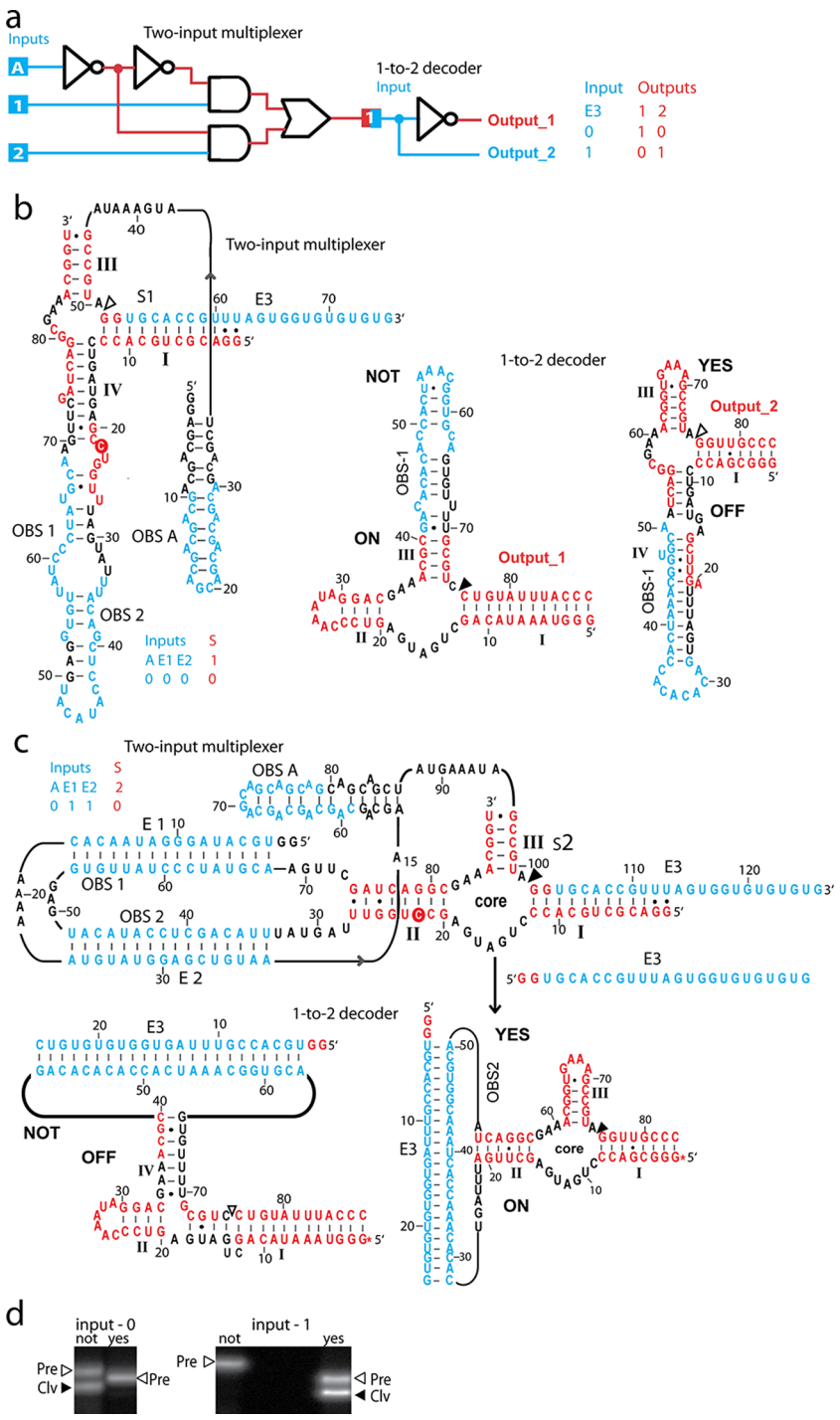

Figure 5. Molecular multiplexer−decoder circuit. (a) A two-input multiplexer is coupled with a 1-to-2 decoder. The output signal (E3) of the multiplexer serves as the input signal for the decoder, which has two output signals. The truth table of the decoder is shown. (b) The OR-ribozyme was employed as a molecular multiplexer while one NOT and one YES gate served as a decoder. A S1 target RNA, which carries a substrate domain (in red), OBS A and E3 (in blue) domains, cannot be cleaved be the ribozyme. As a result, the output signal of the multiplexer has a value of "0". Therefore, NOT-ribozyme is self-cleaved, which produce a signal for output_1, while the YES-ribozyme is inactive. (c) In addition to the sequence of S1, the S2 target RNA carries an E2 effector domain as a spacer built of 15 adenine bases. As a result, the S2 molecule is cleaved by the OR-ribozyme, which releases the E3 effector. Both NOT and YES ribozyme have OBS1 domain that is complementary to the E3. Accordingly, the NOT-ribozyme is switched off while the YES-gate is turned on. This generates a signal from the output_2 from the decoder. (d) Denaturing PAGE gel images of the NOT and YES ribozymes are shown after incubation for 30 min. Each ribozyme was 5′-FAM-ApG labeled. All logic states of the decoder were tested as the cleaved ribozymes exactly correspond to the truth table of the decoder in terms of input as well as output (cleaved and intact ribozymes) signals.

OR-ribozymes (Figure 4b) both in the absence (Figure S4a (SI)) and presence (Figure S4d (SI)) of the addressing effector A. In contrast, the target RNA S5, which lacks effector E2 is cleaved only in the presence of the effector A (Figure 4b) because the hairpin structure has to be opened (Figure S4b (SI)) for the formation of the ribozyme core. In the absence of

dx.doi.org/10.1021/sb300053s | ACS Synth. Biol. 2012, 1, 471−482

the effector A, the hairpin of S5 does not allow the formation of the ribozyme core (Figure S4c (SI)), and the target molecule is not cleaved (Figure 4b).

All ribozyme assays described above exactly reassemble the truth table of a two-input multiplexer circuit (Figure 4a). Note that the full logic of the device is embedded into a single allosteric ribozyme in contrast to the electronic version where five logic gates were employed. This represents a high level of integration of molecular logic circuits. All effector domains can easily be altered, which will allow many molecular multiplexers to work in parallel.

Molecular Multiplexer−Decoder Circuit. One of the main problems facing both nanoscience and nanotechnology is the ability to selectively interact with individual nanostructures at a high density. If this issue is not resolved, many of the potential benefits of these emerging fields will remain unutilized. More specifically, this challenge includes problems such as coupling conventional electronics to novel nanodevices and building high density biosensor circuits. Within the field of nanoelectronics, this challenge can be framed as the ability to fabricate and address integrated molecular circuitry at a high density. One of the main advantages of nucleic acids-based computing is the ability to activate or deactivate a particular gate by a specific nucleic acid sequence in the presence of many other gates.

In this section, we demonstrate a selective activation of the RNA-based multiplexer and passing its output signal to a 1-to-2 decoder (Figure 5a). This indicates that we are able to activate selectively our circuits. As a two-input multiplexer we employed the OR-ribozyme described in the previous section. We apply two target RNAs S1 and S2 (Figure 5b,c). Both molecules carry a hairpin OBS A, and a substrate domain, which contents an E3 effector, complementary to OBS of two other gates, one with NOT and one YES logic functions. The S2 carries in addition effector E2, and a space built of 15 adenine bases (Figure 5).

To construct a molecular 1-to-2 decoder, we employ the two simple logic gates. The allosteric domain of the NOT ribozyme was embedded into stem III in contrast to YES the gate, in which the OBS was introduced into stem II. Note that both YES and NOT gates were designed to sense the same E3 effector (Figure 5b,c) that is produced after S2 cleavage.

All reactions were incubated for 30 min as detailed in the Methods. In the presence of S1 molecule, the core of the OR-ribozyme is not formed (Figure 5b). As a result, the target molecule is not cleaved, and the E3 effector is not released. In this case, the NOT gate is self-cleaved, which propagates output_1 from the decoder while the YES gate is inactive (Figure 5d). In contrast, the S2 target is cleaved by the OR-ribozyme, and the E3 effector is released. Therefore, the NOT-ribozyme is inactive while the YES gate is activated (Figure 5d). This switches the second output from the decoder. The demonstrated molecular multiplexer−decoder circuit is very energy efficient since it is based on nucleic acid hybridization and transesterification. This makes about 40 kcal mol^{-1} spent for generating one output signal of the molecular multiplexer.

Conclusions. Despite the existence of many proof-of-principle demonstrations of molecular computing devices both *in vitro* and *in vivo*, the routine engineering of complex nanocircuits[34] is still ineffective compared with the silicon etched technology. This paper presents computational design and experimental validation of precision IMCs based on single allosteric ribozymes that can sense the length of their target molecules. Some of the input and output sequences are embedded into a single RNA molecule. This is not a problem since the ribozymes are in excess to the target RNAs. As a result, the output sequences are able to carry out the signal only after cleavage.

The implementation of IMC with designer ribozymes is not only original but also practical because it represents a complete technology. This technology includes an efficient algorithm for computational design of synthetic ribozymes that can sense the presence of specific RNA molecules, as well as simple biochemical procedures for synthesis and probing. We have already designed high-speed allosteric ribozymes based on the extended version of the hammerhead ribozyme taking into account all tertiary interactions.[22] This could be applied to the RNA length-sensing ribozymes to produce high-speed switches when needed for some *in vivo* applications.

The computational algorithm applied is proven to be highly accurate predicting precisely that a single base substitution will transform the AND logic function of the ribozyme into an OR logic gate. These findings demonstrate once again that RNA is an evolutionarily very flexible molecule[34] and can easily adapt different functionality as a consequence of a single-point mutation. The abilities to predict such mutations give us the opportunities not only to understand in detail the function of these molecules but also to build robust and complex molecular circuits. In addition, the engineered ribozymes presented throughout this work can be programed to seek-and-destroy predefined RNA molecules with a specific length. The ability to sense the length of RNAs gives a new dimension for utilizing of molecular biosensors. This knowledge can be used not only for various computing applications but also for RNA-based diagnostics of many genetic diseases associated with various tandem repeat expansions such as OPMD disorder.[31]

The paper demonstrates that a single allosteric ribozyme can be programmed to interact with various signal RNA and DNA molecules and to work as integrated digital circuits. Such computing devices can have the functionality of electronic circuits built from up to five logic gates. The achieved functional integration avoids the need for passing and amplifying signals within the integrated circuit, which increases the scalability of this approach compared to schemes based only on interactions among individual logic gates. In contrast to the electronic devices in which the in- and outputs have binary states, the presented ribozymes have a practically unlimited number of digital signals. Therefore, the application of IMCs allows the creation of complex molecular devices working in parallel. The multiplexer−decoder circuit demonstrates our IMCs can talk to each other. We can selectively activate our ribozyme-based IMCs and can read out their signals. Since the target RNAs are separate molecules, the ribozymes can work under multiple turnover conditions amplifying the output signals if needed.

In contrast to many other methods for self-assembly of nucleic acids used for computation, the IMCs presented can propagate their output signals to other molecular gates. As a result, these IMCs are easy for readout. The demonstrated molecular circuits are extremely energy efficient since the signals are generated by RNA hybridization and trans-esterification only. This work makes even more evident that nucleic acids are very suitable media for engineering molecular switches.[34,35] Moreover, it is very easy to reconfigure our allosteric RNA sensors to execute not only other logic function but also a completely different integrated circuit.

Therefore, the presented RNA length sensing ribozymes can be used for RNA-based diagnostics as well as scaling up molecular computation including in microflow reactors.[36] Moreover, in contrast to the deoxyribozymes, the ribozymes can be expressed in the cell for targeting specific RNAs. Such designer ribozymes should be based on the extended version of the hammerhead ribozyme that can work in the cell. This may be of interest for developing future gene therapy methods[37] as well as novel applications in the field of RNA synthetic biology.[38]

■ ASSOCIATED CONTENT

Supporting Information

Figures S1–S4. This material is available free of charge via the Internet at http://pubs.acs.org.

■ AUTHOR INFORMATION

Corresponding Author

*E-mail: robert.penchovsky@hotmail.com. Phone/Fax: +35928167340.

Notes

The authors declare no competing financial interest.

■ ACKNOWLEDGMENTS

This research is funded by a Grant DDVU02/5/2010 awarded by the Bulgarian National Science Fund (BNSF). We also thank Ronald R. Breaker, Yale University, for helpful discussions and Gergana T. Kostova, Sofia University, for assistance with figure preparation.

■ REFERENCES

(1) Nissen, P., Hansen, J., Ban, N., Moore, P. B., and Steitz, T. A. (2000) The structural basis of ribosome activity in peptide bond synthesis. *Science 289*, 920–930.
(2) Cech, T. R. (2000) Structural biology. The ribosome is a ribozyme. *Science 289*, 878–879.
(3) Winfree, E., Liu, F., Wenzler, L., and Seeman, N. C. (1998) Design and self-assembly of two-dimensional DNA crystals. *Nature 394*, 539–544.
(4) Mead, C., and Conway, L. (1980) *Introduction to VLSI Systems*, Addison-Wesley, Boston, MA.
(5) Hodges, D. A., Jackson, H. G., and Saleh, R. (2003) *Analysis and Design of Digital Integrated Circuits*, McGraw-Hill, New York.
(6) Adleman, L. M. (1994) Molecular computation of solutions to combinatorial problems. *Science 266*, 1021–1024.
(7) Stojanovic, M. N., Mitchell, T. E., and Stefanovic, D. (2002) Deoxyribozyme-based logic gates. *J. Am. Chem. Soc. 124*, 3555–3561.
(8) Stojanovic, M. N., and Stafanovic, D. A. (2003) Deoxyribozyme-based molecular automaton. *Nat. Biotechnol. 21*, 1069–1074.
(9) Stojanovich, M. N., and Stefanovich, D. (2003) Deoxyribozyme-based half-adder. *J. Am. Chem. Soc. 125*, 6673–6676.
(10) Lederman, H., Macdonald, J., Stefanovic, D., and Stojanovic, M. N. (2006) Deoxyribozyme-based three-input logic gates and construction of a molecular full adder. *Biochemistry 45*, 1194–1199.
(11) Frezza, B. M., Cockroft, S. L., and Reza Ghadiri, M. (2007) Modular multi-level circuits from immobilized DNA-based logic gates. *J. Am. Chem. Soc. 129*, 14875–14879.
(12) Yashin, R., Rudchenko, S., and Stojanovic, M. N. (2007) Networking particles over distance using oligonucleotide-based devices. *J. Am. Chem. Soc. 129*, 15581–15584.
(13) Elbaz, J., Wang, F., Remacle, F., and Willner, I. (2012) pH-Programmable DNA logic arrays powered by modular DNAzyme libraries. *Nano Lett.*, DOI: 10.1021/nl300051g.
(14) Zhang, D. V., and Erik Winfree, J. (2008) Dynamic allosteric control of noncovalent DNA catalysis reactions. *J. Am. Chem. Soc. 130*, 13921–13926.
(15) Zhang, D. Y., Turberfield, A. J., Yurke, B., and Winfree, E. (2007) Engineering entropy-driven reactions and networks catalyzed by DNA. *Science 318*, 1121–1125.
(16) Elbaz, J., Lioubashevski, O., Wang, F., Remacle, F., Levine, R. D., and Willner, I. (2010) DNA computing circuits using libraries of DNAzyme subunits. *Nat. Nanotechnol. 5*, 417–422.
(17) Qian, L., and Winfree, E. (2011) Scaling up digital circuit computation with DNA strand displacement cascades. *Science 332*, 1156–115.
(18) Forster, A. C., and Symons, R. H. (1987) Self-cleavage of plus and minus RNAs of a virusoid and a structural model for the active sites. *Cell 49*, 211–220.
(19) Ferbeyre, G., Smith, J. M., and Cedergren, R. (1998) Schistosome satellite DNA encodes active hammerhead ribozymes. *Mol. Cell. Biol. 18*, 3880–3888.
(20) Soukup, G. A., and Breaker, R. R. (1999) Engineering precision RNA molecular switches. *Proc. Natl. Acad. Sci. U.S.A. 96*, 3584–3589.
(21) Tang, J., and Breaker, R. R. (1997) Rational design of allosteric ribozymes. *Chem. Biol. 4*, 453–459.
(22) Penchovsky, R., and Breaker, R. R. (2005) Computational design and experimental validation of oligonucleotide-sensing allosteric ribozymes. *Nat. Biotechnol. 23*, 1424–1433.
(23) Margolin, A. A., and Stojnovich, M. N. (2005) Boolean calculations made easy (for ribozymes). *Nat. Biotechnol. 23*, 1374–1376.
(24) Eisenstein, M. (2005) "Computational evolution" offers riboswitch solution. *Nat. Methods 2*, 894.
(25) Sobczak, K., de Mezer, M., Michlewski, G., Krol, J., and Kryzoslak, W. J. (2003) RNA structure of trinucleotide repeats associated with human neurological diseases. *Nucleic Acids Res. 31*, 5469–5482.
(26) Jasinska, A., Michlewski, G., de Mezer, M., Sobczak, K., Kozlowski, P., Napierala, M., and Kryzosiak, W. J. (2003) Structures of trinucleotide repeats in human transcripts and their functional implications. *Nucleic Acids Res. 31*, 5463–5468.
(27) McCaskill, J. S. (1990) The equilibrium partition function and base pair binding probabilities for RNA secondary structure. *Biopolymers 29*, 1109–1119.
(28) Hofacker, I. L., Fontana, W., Stadler, P. F., Bonhoeffer, S., Tacker, M., and Schuster, P. (1994) Fast folding and comparison of RNA secondary structures. *Monatsh. Chem. 125*, 167–188.
(29) Mathews, D., Sabina, J., Zucker, M., and Turner, H. J. (1999) Expanded sequence dependence of thermodynamic parameters improves prediction of RNA secondary structure. *Mol. Biol. 288*, 911–940.
(30) Langlois, M.-A., Lee, N. S., Rossi, J. J., and Puymirat, J. (2003) Hammerhead ribozyme-mediated destruction of nuclear foci in myotonic dystrophy myoblasts. *Mol. Therapy 7*, 670–680.
(31) Blumen, S. C., Brais, B., Korczyn, A. D., Medinsky, S., Chapman, J., Asherov, A., Nisipeanu, P., Codère, F., Bouchard, J.-P., Fardeau, M., Tomé, F. M. S., and Rouleau, G. A. (1999) Homozygotes for oculopharyngeal muscular dystrophy have a severe form of the disease. *Ann. Neurol. 46*, 1531–8249.
(32) Penchovsky, R., and Ackermann, J. (2003) DNA library design for molecular computation. *J. Comp. Biol. 10*, 215–229.
(33) Orr, H. T., and Zoghbi, H. Y. (2007) Trinucleotide repeat disorders. *Annu. Rev. Neurosci. 30*, 575–621.
(34) Bath, J., and Turberfield, A. J. (2007) DNA nanomachines. *Nat. Biotechnol. 2*, 275–284.
(35) Ellington, A. D. (2007) What's so great about RNA? *Chem. Biol. 2*, 445–448.
(36) Penchovsky, R., Birch-Hirschfeld, E., and McCaskill, J. (2000) End-specific covalent photo-dependent immobilization of synthetic DNA to paramagnetic beads. *Nucleic Acids Res. 28*, e98.
(37) Penchovsky, R. (2011) Engineering gene control circuits with allosteric ribozymes in human cells as a medicine of the future. *Quality*

Assurance in Healthcare Service Delivery, Nursing and Personalized Medicine: Technologies and Processes, pp 71−92, IGI Global, Hershey, PA.

(38) Isaacs, J. F., Dwyer, D. J., and Collins, J. J. (2006) RNA synthetic biology. *Nat. Biotechnol. 6,* 545−554.